

New approaches to the quantum-mechanical treatment of charge polarization in intermediate-energy electron scattering

Kunizo Onda and Donald G. Truhlar

Department of Chemistry, University of Minnesota, Minneapolis, Minnesota 55455

(Received 27 December 1979)

Two new approaches to the inclusion of target charge-polarization effects in electron-scattering calculations are presented and tested. The first approach is an energy-dependent polarization potential based on an r^{-6} nonadiabatic correction to the adiabatic polarization potential. The second approach is a matrix effective potential which includes the nonadiabatic dynamics of the polarization effect at all r . The two approaches are tested by comparing them to accurate phase shifts and differential cross sections for electron-helium scattering for impact energies 12–400 eV.

I. INTRODUCTION

At high energies (impact energies at least an order of magnitude greater than the kinetic energies of the relevant bound electrons), electron scattering by atoms or molecules can be described by the first Born approximation. This assumes unpolarized bound states for the target and undistorted-plane-wave states for the scattering electron, which is assumed distinguishable from the bound electrons. At intermediate energies (impact energies 1–10 times the kinetic energies of the relevant bound electrons) one must include the effects of polarization, distortion, and the Pauli principle.¹ Distortion effects can be accounted for by computing the scattering electron wave function numerically in an effective-potential context or a coupled-radial-equations formalism. The effects of the Pauli principle can be included by antisymmetrizing or by using energy-dependent local exchange potentials; in some cases orthogonality constraints on the scattering electron wave function may also be required. Charge polarization of the target is the hardest effect to include realistically. There are two categories of approaches: coupled equations and effective potentials. The coupled-equations methods are generally based on an expansion of the system wave function in products of target states (approximate eigenstates or pseudostates) times scattering electron wave functions, with the latter to be determined by numerical integration or a linear algebraic method.^{2–7} In this kind of approach the numerical solution is expected to involve many target states at low energy but only one target state at energies high enough for the Born approximation to be valid. The target states may be chosen either as (approximate) target eigenstates² or as a combination of eigenstates and pseudostates.^{3–7} The effective-potential approaches treat the scattering event as a single-electron problem with all the many-electron aspects folded into the effective potential.^{8–15}

For the present discussion, “polarized-orbital” methods may be grouped together with effective-potential methods.^{9,16,17} If an effective potential is to represent the decreasing importance of polarization effects as the energy increases, it must be energy dependent. Since polarization and exchange have different characteristics, the energy dependence of the exchange potential alone is insufficient. We will call the interaction of the scattering electron with the unperturbed target the static potential and the difference between the full effective potential and the sum of the static and exchange potentials the polarization potential. So far there has been little work on energy-dependent polarization potentials.

In the present paper we propose two new methods for including energy-dependent polarization effects in electron scattering, and we test them both by applying them to electron-helium scattering. The methods are designed to include the dominant physical effects of energy-dependent polarization but also to be simple enough to be applied to electron-molecule scattering at intermediate energy. We use electron-helium scattering rather than electron-molecule scattering as a test case because recent work has led to both accurate values of the phase shifts at low energy and accurate differential cross sections at intermediate energy.^{7,18–25} For no molecular system have theory and experiment converged so conclusively on accurately known results that can be used to test approximate theories.

The two new approaches proposed and tested here are an energy-dependent polarization potential (EDPP) and a matrix effective potential (MEP). These methods are presented in Sec. II. Since there are frequent reviews in this field, we do not compare our methods and results here to all the previous relevant work; rather we assume that the reader is familiar with standard and recent reviews and we defer to future reviews the task of an overview including the newest methods.

Throughout the article all equations are in hartree atomic units (a.u.), in which $\hbar = m_e = a_0 = e = 1$ and the impact energy of the electron is $k_i^2/2$ or $v^2/2$ where k_i is the initial wave number and v the initial speed. The unit of energy is the hartree (E_h).

II. THEORY

A. Energy-dependent polarization potential (EDPP)

The large- r form of the polarization potential is dominated by the dipole interaction. The leading term is given correctly by the adiabatic approximation which yields (for electron scattering by an atom²⁶⁻³¹)

$$V^{Pa(d1)}(r) \underset{r \rightarrow \infty}{\sim} -\alpha/2r^4, \quad (1)$$

where $V^{Pa(d1)}(r)$ is the adiabatic dipole polarization potential, α is the static dipole polarizability, and r is the distance of the scattering electron from the atomic nucleus. The static dipole polarizability is given correctly by second-order perturbation theory as³²

$$\alpha = \sum_{n \neq 1}^{\infty} \frac{2|\mu_{n1}|^2}{\omega_n}, \quad (2)$$

where μ_{n1} is the transition dipole matrix element connecting the ground state ($n=1$) to excited state n , and ω_n is the excitation energy of state n . In this section we use the average-energy approximation in which

$$\alpha = 2S/\omega, \quad (3)$$

$$S = \sum_{n \neq 1} |\mu_{n1}|^2, \quad (4)$$

and ω is an average excitation energy. In applying this, one approximates the average excitation energy on physical grounds and chooses S so that Eq. (2) yields the correct static dipole polarizability.

The r^{-6} term in the expansion of the dipole polarization potential comes from nonadiabatic effects, and it has been derived by Steenman-Clark and Drachman. Making the average-energy approximation yields³³⁻³⁵

$$V^{P(d1)}(r) \underset{r \rightarrow \infty}{\sim} -\frac{S}{\omega r^4} + \frac{3S}{\omega^2 r^6} + \frac{6Sv^2}{\omega^3 r^6}, \quad (5)$$

where $V^{P(d1)}(r)$ is the dipole polarization potential including both adiabatic and nonadiabatic terms, and v is the incident speed. (Note: in atomic units the incident speed equals the incident wave number k_i for electron scattering.) Putting Eqs. (1), (3), and (5) together yields

$$V^{P(d1)}(r) \underset{r \rightarrow \infty}{\sim} V^{Pa(d1)}(r) \left(1 - \frac{3\omega + 6v^2}{\omega^2 r^2}\right). \quad (6)$$

Equation (6) provides a relation between the large- r forms of the full polarization potential $V^P(r)$ and its adiabatic approximation $V^{Pa}(r)$ that is strictly valid only in the dipole approximation. But the polarization effect is most important at large r , where the dipole terms dominate. At small r the static-exchange potential is more important than the polarization potential. Thus it is interesting to test whether the results are sensitive to the way the polarization potential is continued to small r . There are many possible ways to extend (6) to the full polarization potential $V^P(r)$ including all multipole terms at large r and not making the multipole expansion at small r . We seek a form for $V^P(r)$ that is as simple as possible but agrees with (6) through the two leading terms in the dipole approximation. Two such forms are

$$\text{I} \quad V^P(r) = V^{Pa}(r)/(1 + 6v^2/\omega^2 r^2), \quad (7)$$

$$\text{II} \quad V^P(r) = V^{Pa}(r) \exp(-6v^2/\omega^2 r^2). \quad (8)$$

Expanding Eqs. (7) and (8) yields the first and third terms of (6). For He, at the energies considered in this article and with ω approximated by the ionization potential, $6v^2$ exceeds 3ω by factors of 2 to 65. Thus the third term dominates the second term, and we used the simple expressions (7) and (8) to examine the kinds of results that can be obtained by including the dominant energy-dependent term in the polarization potential.

Similar approximations were suggested in a thesis³⁶ by one of the authors but are tested for the first time here. In the thesis a derivation based on the high-energy impact-parameter method³⁷ was presented; it suggested Eq. (7) but with³⁸ $4v^2/\omega^2$ replacing $6v^2/\omega^2$. We used this to motivate our original choice of ω ; i.e., we approximated $6v^2/\omega^2$ by $4v^2/I^2$ where I is the ionization potential. This yields $\omega = 30$ eV ($1.1018E_h$). Since this is somewhat arbitrary, we also tried repeating the calculations with ω twice as large. We show below that the results are not very sensitive to changing ω even by a factor of 2. Thus our original choice of ω is good enough to illustrate the kind of results that can be obtained with this form of polarization potential.

B. Matrix effective potential (MEP)

The most systematic practical way to mimic charge-polarization effects is to represent the target by a superposition of configurations that allows for the possibility of charge polarization. The coefficients of the various configurations can then be determined as a function of r by a

coupled-channels calculation for each impact energy of interest. This provides a full dynamical treatment of polarization and the results will automatically tend correctly to the limits of adiabatic polarization at large r and low E and no polarization at small r and high E . This treatment can be made to yield the exact results if the target basis is large enough. In practice the target basis must be truncated and one often chooses target-basis functions that explicitly exhibit some particular aspect of target charge polarization, e.g., dipole polarization³⁻⁵ or electron-target short-range correlation.^{6,7} One particularly successful approach for electron-atom scattering has been the use of pseudostates chosen to optimize the target static dipole polarizability α . This ensures that the effective interaction potential is correct at large r and low E . Such α -optimized pseudostates lead to an effective potential that is arbitrary at small distances. This arbitrariness is not important if the α -optimized pseudostates are augmented by other target functions chosen to represent the short-range interaction or if the scattering results of interest are dominated by the long-range forces. These conditions are not always met. The present procedure is designed to include the polarization effect by a coupled-channels treatment, but to simplify the treatment as well as to eliminate the arbitrariness of the effective potential at small r . Whereas the pseudostate procedure can be justified on a variational basis, the matrix effective potential introduced here is justified by a perturbational argument. Another important difference between the approaches relates to economy. For an atom with an S ground state, a P pseudostate yields two pseudochannels coupled to the ground state, but includes only dipole-type polarization and in fact only part of that (even if it is chosen to yield 100% of the static dipole polarizability it does not yield 100% of even the dipole part of the adiabatic polarization potential at any finite r). In contrast, the present procedure involves only one pseudochannel but is designed so that in the adiabatic limit it accounts for 100% of the sum of all multipole contributions to the adiabatic polarization potential at every r . Just as the results of the pseudostate method can be systematically improved by including many pseudostates, the present approach can be systematically improved by increasing the number of pseudochannels. Although a multipseudochannel model would still yield 100% of the adiabatic polarization potential in the adiabatic limit, the additional flexibility could be used to try to improve the representation of the spectrum of response times so that the non-adiabatic effects would be more accurate.

Consider a set of N coupled channels with channel radial functions obeying the differential equations

$$\left(-\frac{d^2}{dr^2} + \frac{L_i(L_i+1)}{r^2} - k_i^2\right)f_i(r) = -2 \sum_{j=1}^N V_{ij}(r)f_j(r). \quad (9)$$

Using second-order perturbation theory and the adiabatic approximation, the polarization potential in channel 1 is given by²⁷⁻³¹

$$V^{Pa}(r) = \sum_{j \neq 1} \frac{|V_{1j}(r)|^2}{\omega_j}. \quad (10)$$

Thus we choose $N=2$,

$$V_{12}(r) = [V^{Pa}(r)\omega]^{1/2}, \quad (11)$$

and

$$k_2^2 = k_1^2 - 2\omega. \quad (12)$$

In Eq. (11), $V^{Pa}(r)$ is the correct adiabatic polarization potential as determined by a separate calculation (see, e.g., Refs. 9 and 15). The two-channel problem with $V_{12}(r)$ and k_2^2 determined by (11) and (12) implicitly includes the correct adiabatic polarization potential at all r through second order in perturbation theory in the adiabatic limit. Having fixed $V_{12}(r)$, however, we abandon second-order perturbation theory and the adiabatic approximation. In their stead we solve the coupled equations (9) numerically, just as if the potential matrix had been calculated from actual target states or pseudostates. Since we have modeled the 2×2 matrix effective potential $V(r)$ rather than the scalar effective potential⁸⁻¹⁵ $V^P(r)$ or the pseudostate wave functions³⁻⁵ $\phi_j(\vec{q})$, we call this the matrix-effective-potential (MEP) method.

To complete the model we must specify $V_{22}(r)$, ω , and L_2 . Since the model yields the correct second-order adiabatic polarization potential for any values of these quantities, we simply give them reasonable values. For the diagonal potential in the pseudochannel we used the simple approximation

$$V_{22}(r) = V_{11}(r). \quad (13)$$

$V_{11}(r)$ is the sum of the static potential and the effective exchange potential for the target ground state. Thus $V_{22}(r)$ also includes static and exchange terms, but $V_{12}(r)$ does not include exchange effects. Notice that we could actually calculate $V_{22}(r)$ and $V_{12}(r)$ if we assumed a target wave function in the pseudochannel instead of modeling the matrix effective potential. But no single r -independent target pseudostate yields the full polarization effect at all r , even in the second-order adiabatic approximation, as our model does.

Thus such a calculation would not be consistent with our model. If $V_{12}(r)$ were calculated from a pseudostate it would be possible to include exchange effects in it by using effective exchange potentials.³⁹

In the same spirit as (13), we assign $l_2 = l_1$. This may be considered a centrifugal sudden approximation⁴⁰ for electronic response. Notice that $l_2 = l_1 \pm 1$ is required for dipole coupling, which dominates at large r . Thus this centrifugal sudden approximation might seriously affect the differential cross section. However, the model yields the correct second-order adiabatic polarization potential for any value of l_2 , and the adiabatic term dominates at large r ; thus the large- r scattering is independent of l_2 through second order. The use of an average value $l_2 = l_1$ is even more justified at smaller r , where many multipole terms contribute importantly, and at very large r , where the scattering comes from very large l ($l \gg 1$). To include two pseudochannels, for example, one with $l_2 = l_1 - 1$ and one with $l_2 = l_1 + 1$, would certainly allow the model to be more accurate. However, the first goal of the present study is to learn how accurately we can treat the problem with a single "average" pseudochannel.

A reasonable choice for ω is the average excitation energy. If most of the polarization came from a single state with excitation energy ω , then this choice would ensure a correct response time for the system and make the treatment of non-adiabatic effects realistic. Of course, real systems have a spectrum of excitation energies and response times. The goal of the present work is to see how accurately we can model the true polarization response of the system with a single pseudochannel and hence a single ω . Thus we set ω equal to an average excitation energy. For most of the calculations we set the average excitation energy equal to the ionization potential 24.481 eV ($\omega = 0.89971 E_h$). For some phase shifts we tried other values to test the sensitivity.

III. CALCULATIONS

The static potential and target electron density are taken from the compilation of Strand and Bonham,⁴¹ who presented analytic fits to the Hartree-Fock results of Roothaan *et al.*⁴² The exchange potential is evaluated using the semi-classical exchange approximation.⁴³

The adiabatic polarization potential was calculated from the expression derived by Dalgarno and Lynn.⁴⁴ Their expression results from second-order perturbation theory when the target is treated in the Hartree-Fock approximation with hydrogenic orbitals. The effective nuclear charge

in the hydrogenic orbitals was set equal to 1.5971 so that the static dipole polarizability comes out equal to its accurate value⁴⁵ 1.383 19 a.u. The use of second-order perturbation theory is consistent with the derivation of Eq. (11) and is accurate at large r where Eq. (6) is applicable. Nevertheless, a finite-field variational calculation¹⁵ yields a more accurate adiabatic polarization potential at small r and might be preferred on those grounds.

The single-channel and two-channel Schrödinger equations were solved by our variable-step-size Numerov program.⁴⁶ The differential cross sections for elastic scattering were computed from the phase shifts for the single-channel methods and from the T -matrix elements for the MEP method. To converge the differential cross sections, we augmented the numerically calculated phase shifts and T -matrix elements for small l ($l \leq l_{(1)}$) by asymptotic polarized Born phase shifts for large l ($l_{(1)} < l \leq l_{(2)}$). The polarized Born approximation⁴⁷ is the first Born approximation applied to potential scattering by an effective potential including a polarization term. In the asymptotic polarized Born approximation, valid at high enough l , the effective potential is replaced by the asymptotic form (1). Using the partial-wave Born approximation⁴⁸ for a diagonal element of the reactance matrix, one obtains for the phase shift

$$\eta_l = \tan^{-1} \frac{\pi \alpha k^2}{(2l+3)(2l+1)(2l-1)}, \quad l \geq 1. \quad (14)$$

For each energy, $l_{(1)}$ and $l_{(2)}$ were chosen large enough so that the differential cross section was well converged with respect to increasing either of them. The values finally used are given in Table I. We also calculated differential cross sections in the static-exchange approximation for comparison. For the static-exchange calculations we set $l_{(1)} = l_{(2)} = 15$ for all energies.

In the MEP method, the phase shifts are complex; i.e.,

$$\eta_l = \delta_l + i\gamma_l. \quad (15)$$

The integral cross sections for elastic, inelastic, and total (elastic plus inelastic) scattering are then given by⁴⁹

$$\sigma_{el} = \pi k^{-2} \sum_l (2l+1) |1 - S_{11}^l|^2, \quad (16)$$

$$\sigma_{inel} = \pi k^{-2} \sum_l (2l+1) (1 - |S_{11}^l|^2), \quad (17)$$

$$\sigma_{tot} = \sigma_{el} + \sigma_{inel} = 2\pi k^{-2} \sum_l (2l+1) (1 - \text{Re} S_{11}^l), \quad (18)$$

TABLE I. Angular-momentum limits for differential cross sections.

E (eV)	$l_{(1)}$	$l_{(2)}$
12-19	10	50
30-50	20	50
100	30	70
200	40	100
400	60	140

where

$$S_{11}^I = \exp(2i\eta_I). \quad (19)$$

IV. RESULTS

In presenting the results we sometimes use the following abbreviations. S: static approximation;

SE: static-exchange approximation; MEP: matrix-effective-potential method; APB: asymptotic polarized Born approximation; SEPa: static-exchange-plus-adiabatic-polarization approximation; SEPna: static-exchange-plus-nonadiabatic-polarization approximation. Two kinds of non-adiabatic polarization potential are considered. EP: extended polarization approximation^{17, 35, 50-52}; EDPP: energy-dependent polarization potential.

The calculated phase shifts for the s , p , and d waves are given in Tables II-IV. They are compared to accurate phase shifts determined by phase-shift analyses^{18, 24} of experimental results and by accurate calculations.^{7, 53} We also compare the present results to previous ones obtained in the static,⁴³ static-plus-semiclassical-exchange,⁴³ static-plus-Hartree-Fock-exchange,^{54, 55} and ex-

TABLE II. s -wave phase shifts (rad).^a

E (eV)	S	SE	SEPa	SEPna ^b	MEP ^c	Accurate
12	1.437	1.913	2.174	I: 1.956 II: 1.940 I': 1.994	2.223 2.263	1.985 ^d 1.968 ^e 1.989 ^f
13.6	1.406 1.405 ^g	1.857 1.856 ^g 1.890 ^h 1.888 ⁱ	2.119	I: 1.896 II: 1.880 I': 1.933 EP: 1.955	2.181 2.241	1.936 ^f 1.955 ^j
19	1.324	1.704	1.969	I: 1.735 II: 1.720 I': 1.769	2.133 3.257	1.814 ^d 1.800 ^e 1.803 ^f
30	1.214	1.500	1.759	I: 1.521 EP: 1.611	1.720 + $i0.123$ 1.711 + $i0.134$	
30.6	1.210	1.492 1.522 ^h	1.750	I: 1.512	1.712 + $i0.123$ 1.702 + $i0.135$	
50	1.095	1.290	1.529	I: 1.302 EP: 1.391	1.478 + $i0.136$ 1.454 + $i0.142$	
54.4	1.076	1.257 1.279 ^h	1.492	I: 1.268 II: 1.259 I': 1.287	1.435 + $i0.136$ 1.410 + $i0.142$	
100	0.942	1.046	1.245	I: 1.051 EP: 1.112	1.149 + $i0.117$ 1.131 + $i0.114$	
200	0.799	0.849	1.004	I: 0.851 EP: 0.868	0.896 + $i0.078$ 0.888 + $i0.072$	
400	0.668	0.691	0.807	I: 0.692 EP: 0.687	0.712 + $i0.047$ 0.708 + $i0.042$	

^a Results are from the present calculations except where indicated otherwise. S denotes only static potential, SE denotes only static and exchange potentials, SEPa denotes SE plus adiabatic polarization potential, SEPna denotes SE plus full polarization potential including nonadiabatic effects.

^b I: EDPP, Eq. (7), ω equals 30 eV; II: EDPP, Eq. (8), ω equals 30 eV; I': EDPP, Eq. (7), ω equals 60 eV; EP: extended polarization model.

^c Top entry: ω equals ionization potential; bottom entry: ω equals 2^1P excitation energy.

^d Andrick and Bitsch, Ref. 18.

^e Williams, Ref. 24.

^f Nesbet, Ref. 7.

^g Riley and Truhlar, Ref. 43.

^h Duxler, Poe, and LaBahn, Ref. 54.

ⁱ Burke and Robb, Ref. 55.

^j Sinfaiam and Nesbet, Ref. 53.

TABLE III. p -wave phase shifts (rad).^a

E (eV)	S	SE	APB	SEPa	SEPna ^b	MEP ^c	Accurate
12	0.053	0.193	0.250	0.374	I: 0.259 II: 0.236 I': 0.309	0.361 0.359	0.259 ^d 0.242 ^e 0.243 ^f
13.6	0.061 0.060 ^g	0.206 0.205 ^g 0.183 ^{h,i}	0.282	0.395	I: 0.268 II: 0.242 I': 0.320 EP: 0.251	0.382 0.381	0.263 ^f 0.265 ^j
19	0.086	0.239	0.384	0.446	I: 0.288 II: 0.258 I': 0.342	0.437 0.440	0.325 ^d 0.311 ^e 0.316 ^f
30	0.130	0.278	0.568	0.493	I: 0.308 EP: 0.336	0.516 + i 0.020 0.518 + i 0.043	
30.6	0.133	0.280 0.284 ^h	0.578	0.494	I: 0.309	0.519 + i 0.023 0.519 + i 0.046	
50	0.187	0.311	0.817	0.517	I: 0.326 EP: 0.352	0.526 + i 0.088 0.507 + i 0.105	
54.4	0.196	0.315 0.327 ^h	0.859	0.518	I: 0.329 II: 0.317 I': 0.394	0.519 + i 0.096 0.498 + i 0.112	
100	0.256	0.336	1.132	0.513	I: 0.342 EP: 0.347	0.452 + i 0.108 0.433 + i 0.109	
200	0.298	0.340	1.340	0.483	I: 0.342 EP: 0.334	0.390 + i 0.077 0.381 + i 0.071	
400	0.308	0.328	1.563	0.438	I: 0.329 EP: 0.319	0.350 + i 0.046 0.345 + i 0.042	

^{a-j} See Table II.TABLE IV. d -wave phase shifts (rad).^a

E (eV)	S	SE	APB	SEPa	SEPna	MEP	Accurate
12	0.004	0.017	0.036	0.056	I: 0.041 II: 0.038 I': 0.050	0.052 0.051	0.037 ^e 0.036 ^f
13.6	0.005 0.005 ^g	0.020 0.020 ^g 0.014 ^{h,i}	0.041	0.063	I: 0.045 II: 0.041 I': 0.046 EP: 0.042	0.059 0.058	0.041 ^f 0.039 ^j
19	0.010	0.029	0.058	0.086	I: 0.054 II: 0.046 I': 0.071	0.081 0.081	0.058 ^e 0.058 ^f
30	0.020	0.047	0.091	0.124	I: 0.068 EP: 0.083	0.126 + i 0.003 0.128 + i 0.009	
30.6	0.021	0.048 0.042 ^h	0.093	0.126	I: 0.068	0.128 + i 0.004 0.130 + i 0.010	
50	0.040	0.072	0.151	0.170	I: 0.086 EP: 0.111	0.173 + i 0.033 0.166 + i 0.041	
54.4	0.044	0.076 0.074 ^h	0.164	0.177	I: 0.089 II: 0.078 I': 0.110	0.178 + i 0.038 0.169 + i 0.046	
100	0.080	0.111	0.295	0.222	I: 0.117 EP: 0.141	0.191 + i 0.064 0.180 + i 0.065	
200	0.125	0.148	0.546	0.255	I: 0.150 EP: 0.159	0.191 + i 0.059 0.183 + i 0.054	
400	0.161	0.174	0.883	0.266	I: 0.175 EP: 0.172	0.195 + i 0.040 0.191 + i 0.037	

^{a-j} See Table II.

tended polarization⁵⁰⁻⁵² approximations. The main reason for the comparison between present static-plus-semiclassical-exchange results and the static-plus-Hartree-Fock-exchange results is to show how much of the error in the present calculations might be due to our treatment of exchange. In general the different treatments of exchange do not lead to large differences in the phase shifts; therefore the discussion in Sec. V will emphasize the differences in the treatment of charge polarization rather than exchange.

The l dependence of the phase shifts for one energy is illustrated in Table V.

One of the most serious assumptions in the MEP model is that the response of the target can be represented in terms of a single pseudochannel. To test this we performed some calculations with two pseudochannels. To do this we replace Eqs. (11) and (12) by

$$\alpha = \sum_{j=2}^N \alpha_j, \quad (20)$$

$$V_{1j}(r) = [(\alpha_j/\alpha) V^{\text{Pa}}(r) \omega_j]^{1/2}, \quad j \neq 1, \quad (21)$$

$$V_{jk}(r) = 0, \quad j \neq k, \quad j \neq 1, \quad k \neq 1, \quad (22)$$

$$k_j^2 = k_1^2 - 2\omega_j. \quad (23)$$

The results for several choices of the pseudochannel parameters are shown in Table VI. Notice that $N=3$ corresponds to two pseudochannels.

The differential cross sections for elastic scattering are shown as functions of scattering angle θ in Figs. 1-7. They are compared to the experimental results of Bromberg,⁵⁶ Andrick and Bitsch,¹⁸ Jansen *et al.*,⁵⁷ Williams,²⁴ and Register *et al.*²⁵ and the accurate calculated results of Nesbet.⁷ In general, in the figures the calculated results are shown as various kinds of curves and are identified in the figure itself. The EDPP results are based on functional form I, Eq. (7), and the average excitation energy is set equal to the 30 eV and the ionization potential for the EDPP and

TABLE V. Phase shifts (rad) for $E=50$ eV.

l	APB	SEPa	EDPP	MEP
0		1.529	1.302	1.478 +i0.136
1	0.817	0.517	0.326	0.526 +i0.088
2	0.151	0.170	0.086	0.173 +i0.033
3	0.0507	0.0657	0.0283	0.0682 +i0.0116
4	0.0230	0.0294	0.0121	0.0310 +i0.0040
5	0.0124	0.0150	0.0065	0.0159 +i0.0014
6	0.0074	0.0085	0.0041	0.0090 +i0.0005
7	0.0048	0.0053	0.0029	0.0056 +i0.0002
10	0.0017	0.0018	0.0012	0.0019 +i0.00001
15	0.00054	0.00055	0.00045	0.00055 +i0.00000
20	0.00023	0.00023	0.00021	0.00024 +i0.00000

MEP models, respectively. In addition to the true MEP results, which are shown as an ordinary curve in Figs. 1 and 2 and a thin curve in Figs. 3-7, Figs. 3-7 show what we obtain if we use the MEP value of the real part of the phase shift but neglect the imaginary part of the phase shift. These $\gamma_l = 0$ results are shown as ordinary curves. The experimental results are identified in the captions rather than the figures. Register *et al.* used a phase-shift analysis to extrapolate their results to 0° and 180° , and their results are shown as short-dashed curves. The other experimental results are shown as various kinds of symbols.

The integral cross sections σ_{el} , σ_{in} , and σ_{tot} and the elastic momentum-transfer cross sections $\sigma_{\text{el}}^{\text{m}}$ are given in Tables VII and VIII. In these tables the present results are compared to the experimental results of Andrick and Bitsch,¹⁸ Milloy and Crompton,¹⁹ Blaauw *et al.*,²⁰ Kennerly and Bonham,²³ and Register *et al.*²⁵ and to the accurate calculated results of Nesbet.⁷ These experimental and calculated results are generally quite consistent and represent a reasonable consensus of the true answers. We also compare to the results of the extended polarization calculations of LaBahn and Callaway^{50,52} since this theory

TABLE VI. Phase shift (rad) for $l=2, 6$, and 10 at $E=50$ eV.

Method	N	(α_2/α)	$h\omega_2$ (eV)	l_2	$h\omega_3$ (eV)	l_3	a	η_2	η_6	η_{10}
SE	1							0.0716	0.00032	0.000002
APB	1							0.1509	0.00744	0.00174
SEPa	1							0.1695	0.00851	0.00181
SEPna ^a	1		29.983					0.0855	0.00411	0.00124
MEP	2	1.00	24.481	l			1.0	$0.1731 + i0.0327$	$0.00899 + i0.00051$	$0.00186 + i0.00001$
MEP	3	0.50	24.481	l	24.481	l	1.0	$0.1731 + i0.0327$	$0.00899 + i0.00051$	$0.00186 + i0.00001$
MEP	3	0.35	21.215	l	26.240	l	1.0	$0.1723 + i0.0327$	$0.00897 + i0.00057$	$0.00186 + i0.00002$
MEP	3	0.50	24.481	$l-1$	24.481	$l+1$	1.0	$0.1255 + i0.1126$	$0.01034 + i0.00247$	$0.00207 + i0.00009$
MEP	2	1.00	24.481	l			2.0	$0.1981 + i0.1523$	$0.00923 + i0.00057$	$0.00186 + i0.00001$

^a EDPP, Eq. (7).

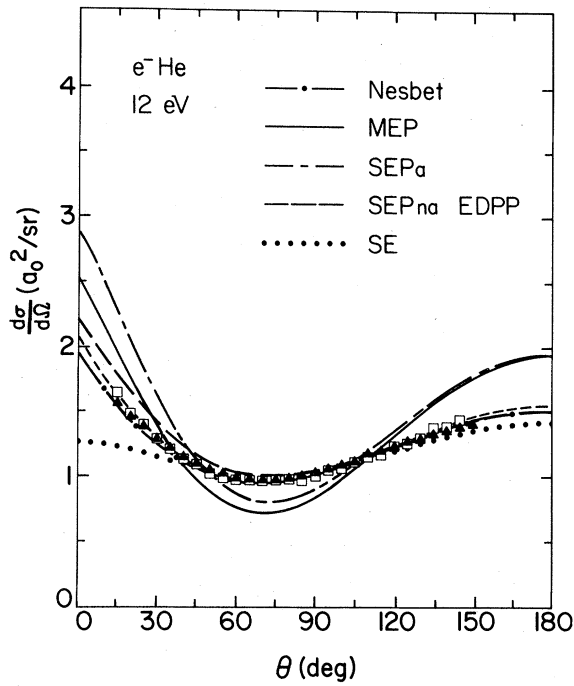


FIG. 1. Differential cross sections at 12 eV. The theoretical results are explained in Sec. IV. The experimental results are: \square , Andrick and Bitsch; \blacktriangle , Williams; ----, Register, Trajmar, and Srivastava.

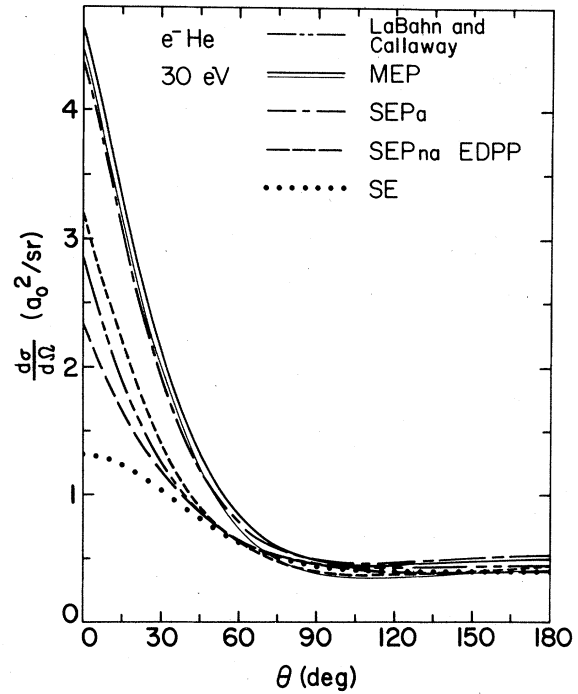


FIG. 3. Differential cross sections at 30 eV. The theoretical results are explained in Sec. IV. The experimental results are: ----, Register, Trajmar, and Srivastava.

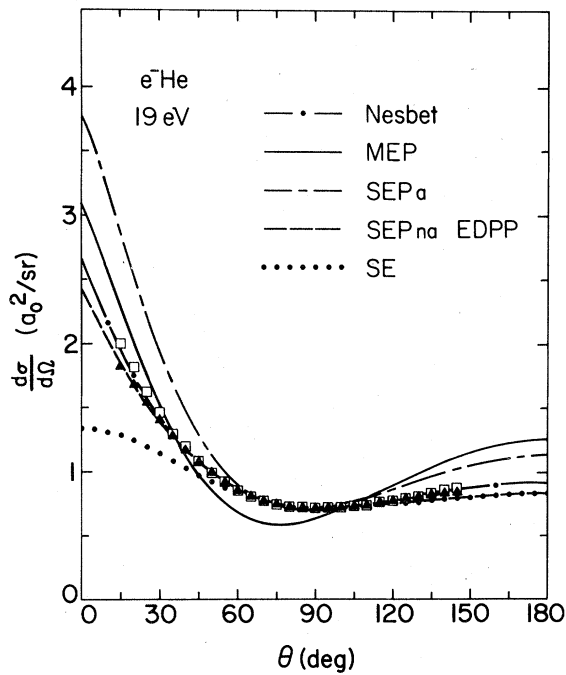


FIG. 2. Differential cross sections at 19 eV. The theoretical results are explained in Sec. IV. The experimental results are: \square , Andrick and Bitsch; \blacktriangle , Williams.

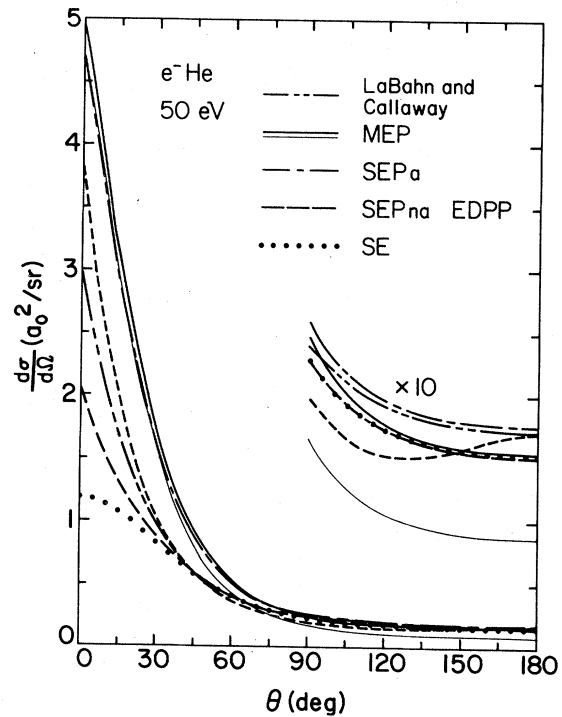


FIG. 4. Differential cross sections at 50 eV. The theoretical results are explained in Sec. IV. The experimental results are: ----, Register, Trajmar, and Srivastava.

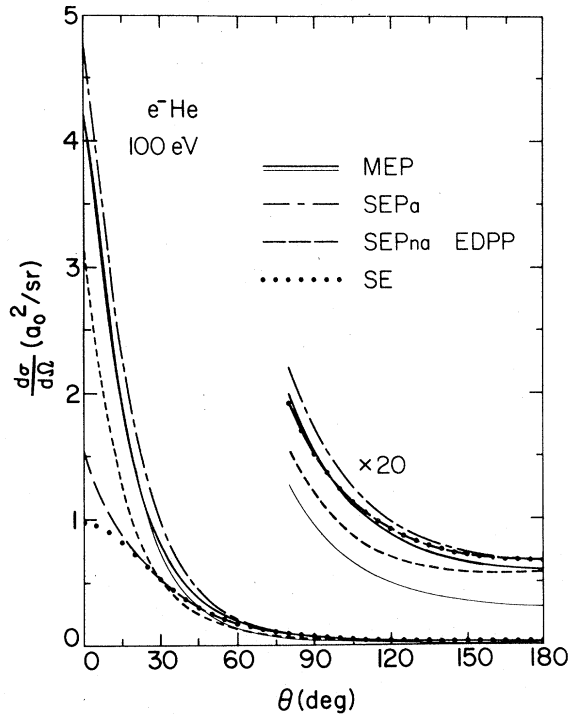


FIG. 5. Differential cross sections at 100 eV. The theoretical results are explained in Sec. IV. The experimental results are: ----, Register, Trajmar, and Srivastava.

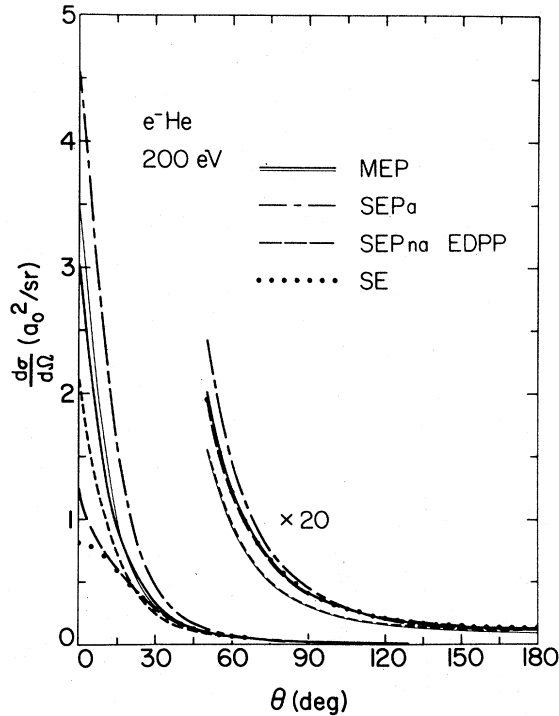


FIG. 6. Differential cross sections at 200 eV. The theoretical results are explained in Sec. IV. The experimental results are: ----, Register, Trajmar, and Srivastava.

has been applied with reasonable success to electron-helium scattering over a wide energy range; and we compare to the static-plus-Hartree-Fock-exchange results of Dewangan and Walters⁵⁸ as a test of the accuracy of the local exchange approximations at high energy. The values of σ_{s1}^a listed for LaBahn and Callaway in Tables VII and VIII were calculated by us from their published phase shifts. Tables VII and VIII also show the values of σ_{s1} , σ_{inel} , and σ_{tot} recommended by deHeer and Jansen²¹ in 1977 on the basis of an evaluation of all available experiments. Register *et al.*²⁵ have summed their own experimental values of σ_{s1} and deHeer and Jansen's σ_{inel} to obtain alternative values of σ_{tot} , and these are also given in the tables for comparison.

V. DISCUSSION OF RESULTS

A. *s*-wave phase shifts

At energies up to 19 eV, we know accurate phase shifts^{7,18,24} to test the approximate theories. The adiabatic model (SEPα, see list of abbreviations at beginning of Sec. IV) yields phase shifts that are too high, indicating that the adiabatic polarization potential is too attractive, as is well known.¹⁷ Surprisingly, the MEP model yields even larger

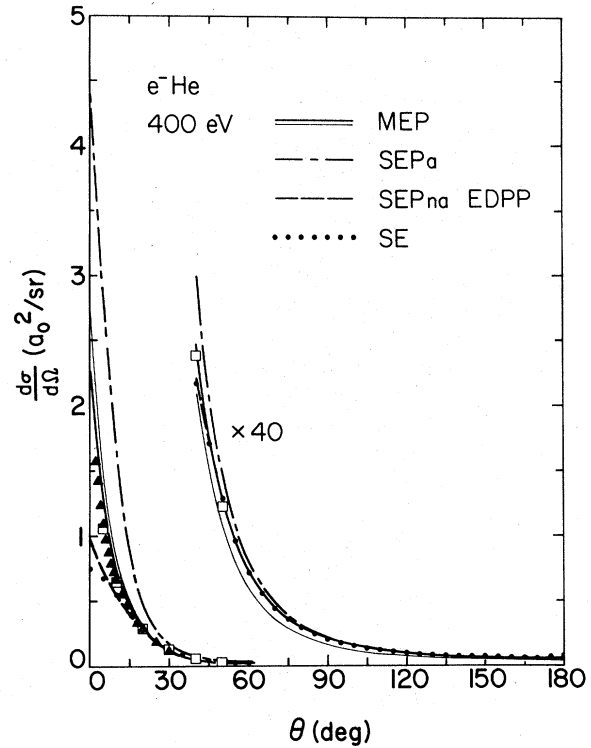


FIG. 7. Differential cross sections at 400 eV. The theoretical results are explained in Sec. IV. The experimental results are: ▲, Bromberg; □, Jansen, deHeer, Luyken, van Wingerden, and Blaauw.

s-wave phase shifts at these energies. In contrast the EDPP model is a considerable improvement over the adiabatic one. It reduces the relative errors in the phase shifts from about 0.2 rad to 0.02–0.08 rad. It is interesting that both the EDPP results and the accurate results are much closer to the no-polarization (SE) results than to the adiabatic ones. The EDPP results are not very sensitive to the form (I vs. II) of the polarization potential at small r or even to doubling the effective excitation energy. Sensitivity to more reasonable variations in the effective excitation energy would be smaller.

At higher energies the MEP phase shift drops below the adiabatic one, and both the MEP and the EDPP tend to the SE result at high energy as expected. The EDPP phase shift is within 0.02 rad of the SE one at all energies above 30 eV. In contrast the MEP phase shift is still halfway between the SE and SEPa ones at 100 eV and approaches the SE phase shift within 0.02 rad only at 400 eV. At 30–50 eV the extended polarization results are midway between the EDPP and the MEP but at 100 eV and higher they are closer to the MEP. The MEP would seem to include the physics more fully than the single-channel EDPP or EP models, but since there are no accurate phase shifts available at these energies, the success and failures of the models at these energies will have to be judged on the basis of the differential and integral cross sections discussed below.

With one exception, the MEP model is not very sensitive to average excitation energy. The exception occurs at 19 eV, which is very close to the pseudothreshold at 21.215 eV. In general one should avoid using pseudostate and pseudochannel models too close to pseudothresholds.^{6,59}

B. Higher phase shifts

The *s*-wave phase is qualitatively different from all the others in that there is no centrifugal potential. This means that the incident electron fully probes the strong short-range potential. For the higher partial waves the centrifugal potential keeps the electron out and the long-range polarization potential is relatively more important. The present calculations illustrate this quantitatively. For example, at 12 eV, the ratio of SEPa to SE phase shifts is 1.14, 1.94, and 3.27 for the *s*, *p*, and *d* waves, respectively. At 50 eV these ratios are 1.19, 1.66, and 2.37, respectively, and at 400 eV they are 1.17, 1.34, and 1.53, respectively. Since the polarization effect is easier to model at large r , the present models should be more successful for the higher partial waves.

Tables II and III show that the EDPP phase shifts (models I and II) are again in remarkably good

agreement with the accurate phase shifts at 12–19 eV. For $l > 0$, the EDPP becomes more sensitive to ω , but even doubling ω (which is an unphysically large change) increases the phase shift by only 0.05 rad. For the *p* wave, the accurate and EDPP phase shifts are closer to the SE results than to the SEPa ones. For the *d* wave the accurate and EDPP phase shifts are about halfway between the SE and SEPa ones. The MEP phase shifts for 12–19 eV are only a little less than the SEPa ones for both the *p* wave and the *d* wave.

At higher energies (30–400 eV), the EDPP and EP phase shifts are relatively close to the SE ones but the MEP phase shifts are closer to the SEPa ones up to 100 eV.

Next consider the convergence of the phase shifts to the asymptotic polarized Born form as l is increased at constant E . Table IV shows that the accurate *d*-wave phase shift is remarkably close to the APB result for $l = 2$ at 12–19 eV. Consideration of the wide range of variation of the SEPa and SEPna results, however, shows that the success of the APB is not due to the satisfaction of the assumptions of its derivation. In other words, when we perform actual calculations with effective potentials that have the correct asymptotic form but we do not assume the asymptotic form at all r and we do not assume free-particle wave functions for the scattering electron, we do not obtain the APB result for every realistic short-range form of the potential. Thus the APB should not be assumed reliable for all $l \geq 2$ just because it happens to be fairly accurate for $l = 2$.

An example of the convergence of the various phase shifts to the results predicted by the asymptotic form is shown in Table V. An interesting point illustrated by this table is that EDPP formalism converges most slowly to the asymptotic limit; this is found to be the case at other energies too. Another interesting point is that the real parts of the MEP phase shifts are not necessarily less than the adiabatic ones.

C. Elastic cross sections at 12–19 eV

The cross sections at 12–19 eV (Figs. 1 and 2 and Table VII) confirm the trends seen above in the comparison with the accurate phase shifts. The static-exchange approximation predicts far too little scattering for $\theta \leq 30^\circ$, but the EDPP is in excellent agreement with experiment at all scattering angles. The MEP and adiabatic models are relatively poor approximations at 12 eV and overestimate the forward scattering and the integral and momentum-transfer cross sections at both 12 and 19 eV.

TABLE VII. Integral and momentum-transfer cross sections (α_0^2) at impact energies 12–50 eV.

E (eV)	12		19		30				50			
	σ_{el}	$\sigma_{\text{el}}^{\text{m}}$	σ_{el}	$\sigma_{\text{el}}^{\text{m}}$	σ_{el}	$\sigma_{\text{el}}^{\text{m}}$	σ_{inel}	σ_{tot}	σ_{el}	$\sigma_{\text{el}}^{\text{m}}$	σ_{inel}	σ_{tot}
Experiment												
Andrick and Bitsch ^a	14.82	15.28	11.39	10.21								
Milloy and Crompton ^b		14.82										
Blaauw <i>et al.</i> ^c								8.52				6.20
deHeer and Jansen ^d					7.98		0.81	8.79	4.95		1.52	6.47
Kennerly and Bonham ^e			14.14					8.43				6.00
Register <i>et al.</i> ^f	14.14	15.25			7.54	5.38		8.36	4.51	2.51		6.04
Theory												
Nesbet ^g	14.49	15.04	11.31	10.15								
LaBahn and Callaway ^h					7.79	5.99			4.81	2.99		
SE	14.23	14.81	10.39	9.69	7.02	5.66			4.21	2.77		
SEPa	15.61	16.37	13.04	11.31	9.85	6.80			6.55	3.38		
EDPP ^{i, j}	15.18	15.40	11.09	9.87	7.42	5.69			4.38	2.77		
MEP ($\gamma=0$) ^k					10.28	6.76			6.64	3.22		
MEP ^k	14.55	15.28	11.62	11.14	8.97	5.49	0.99	9.96	5.52	2.25	2.13	7.65

^a Reference 18.^b Reference 19.^c Reference 20.^d Reference 21.^e Reference 23.^f Reference 25.^g Reference 7.^h Reference 52.ⁱ Equation (7).^j ω equal to 30 eV.^k ω equal to ionization potential.TABLE VIII. Integral and momentum-transfer cross sections (α_0^2) at impact energies 100–400 eV.

E (eV)	100				200				400			
	σ_{el}	σ_{el}^m	σ_{inel}	σ_{tot}	σ_{el}	σ_{el}^m	σ_{inel}	σ_{tot}	σ_{el}	σ_{el}^m	σ_{inel}	σ_{tot}
Experiment												
Blaauw <i>et al.</i> ^a				3.99				2.59				1.65
deHeer and Jansen ^b	2.18		1.89	4.07	0.98		1.65	2.63	0.44		1.16	1.61
Register <i>et al.</i> ^c	2.00	0.75		3.89	0.88	0.22		2.53	0.41			1.57
Theory												
LaBahn and Callaway ^d	2.23	1.00			0.98	0.29			0.44	0.084		
Dewangen and Walters ^e	2.01				0.91				0.42			
SE	1.96	0.93			0.90	0.29			0.42	0.087		
SEPa	3.40	1.14			1.67	0.35			0.81	0.103		
EDPP ^{f,g}	2.01	0.93			0.91	0.29			0.42	0.086		
MEP ($\gamma=0$) ^h	2.88	1.00			1.16	0.30			0.50	0.088		
MEP ^h	2.47	0.68	2.47	4.93	1.07	0.23	1.98	3.05	0.48	0.074	1.37	1.85

^a Reference 20.^b Reference 21.^c Reference 25.^d Reference 50.^e Reference 58.^f Equation (7).^g ω equal to 30 eV.^h ω equal to ionization potential.

D. Elastic cross sections at 30–50 eV

Next consider the 30 and 50 eV cross sections in Figs. 3 and 4 and Table VII. The MEP differential cross section is still close to the adiabatic one for small θ , and thus this model predicts too large a forward peak. The EDPP result is most similar to the EP one, and both these methods underestimate the forward scattering. At both energies, the EP model is closer to experiment than the other three (MEP, SEPa, and EDPP) models. The static approximation is worse than any of them.

At large scattering angles the imaginary part of the MEP phase shift has a much larger effect than for small θ , and it greatly diminishes the MEP differential cross section as expected. Unfortunately, this makes the MEP differential cross section too small at large θ . None of the models is in excellent agreement with the large-angle data at these energies. However, the MEP model is in excellent agreement with the momentum-transfer cross sections, which are most sensitive to medium and large scattering angles.

E. Elastic cross sections at 100–400 eV

Now consider the cross sections in Figs. 5–7 and Table VIII. At these energies neither the SEPa nor the SE differential cross section agrees with experiment within 50% at small θ . At 100 eV the MEP prediction at small angles has improved considerably as compared to lower energies, and it must be considered superior to the EDPP model for small-angle scattering. The MEP model gets even better at 200 and 400 eV. The large-angle differential cross sections predicted by the MEP are also more accurate at these energies than at lower energies; at 200 eV the large-angle cross section predicted by the MEP is better than any of the other models considered. At 100 and 200 eV the MEP model is in good agreement with the momentum-transfer cross sections, whereas the other calculations all lead to too high a value. The good agreement of the MEP results with the experimental momentum-transfer cross sections at 30–200 eV can probably be attributed to taking account of loss of flux into inelastic channels. We shall see in subsection V F that the MEP model does predict the flux loss reasonably accurately.

At energies of 100 eV and higher the EDPP predicts a qualitatively incorrect shape for the small-angle differential cross section, clearly underestimating the polarization effect. Although we included EDPP calculations at these energies for completeness, the expansion assumed for the potential breaks down when $6v^2/\omega^2r^2 \gtrsim 1$. At 100 eV, $6v^2/\omega^2r^2$

$= 36.3/r^2$ so that the model has become inappropriate over an appreciable range of r . The present calculations confirm quantitatively the extent of the inappropriateness of this model at high energy. Actually the SE and EDPP do predict accurate integral elastic cross sections at high energies but this results from a cancellation of errors with the differential cross section being underestimated at small θ and overestimated at large θ .

It is interesting to compare the present EDPP treatment to Hayashi and Kuchitsu's quasiadiabatic polarization potential,⁶⁰ which is also a real-valued, energy-dependent model. Their potential is

$$V^P(r) = \frac{f(r)}{r^4} \sum_n \frac{|\mu_n|^2}{\omega_n} F\left(\frac{v}{\omega_n r}\right), \quad (24)$$

where

$$f(r) = 1 - \exp[-(r/c)^6]. \quad (25)$$

The cutoff function $f(r)$ is an arbitrary form designed to compensate for the breakdown of their model at small r and the resulting singularity at the origin. For He they used $c = 0.57a_0$ and found that changing it by up to 50% made differences of 20% or less in the cross section for energies 100 eV or more.⁶¹ The function $F(v/\omega_n r)$ accounts for nonadiabatic effects as modeled by a target response to a constant-velocity, straight-line-path trajectory.⁶⁰ For electron-helium scattering, this function can be approximated by⁶¹

$$F(x) = \frac{1 + 2.97x^2}{1 + 0.246x^2 + 1.79x^4}. \quad (26)$$

The adiabatic limit in this model is achieved by letting $(v/r) \rightarrow 0$. This yields

$$V^{Pa}(r) = f(r) \sum_n \frac{|\mu_n|^2}{\omega_n r^4}. \quad (27)$$

Combining Eqs. (24) and (27) and making the average-energy approximation yields

$$V^P(r) = V^{Pa}(r) F(v/\omega r) \quad (28)$$

$$r \sim_\infty V^{Pa}(r) \left(1 + \frac{2.72v^2}{\omega^2 r^2}\right). \quad (29)$$

In contrast, model I yields

$$V^P(r) \sim_\infty V^{Pa}(r) \left(1 - \frac{6v^2}{\omega^2 r^2}\right). \quad (30)$$

Thus the leading nonadiabatic effect in the Hayashi-Kuchitsu model has the opposite sign to ours. There are important differences in the way the models have been applied. We propose to use a reasonably accurate $V^{Pa}(r)$, whereas they use Eq. (27). We include exchange whereas they have neglected it.⁶¹ Finally, they do not use the

average-energy approximation. This requires knowing the distribution of oscillator strength or at least some moments of this distribution. When this information is available it could be incorporated into our model as well. Hayashi and Kuchitsu applied their model to electron-helium scattering at 100–500 eV.⁶¹ Their differential cross sections at 0° at 100, 200, and 400 eV are 4.31, 2.97, and $1.97a_0^2$, respectively. Comparison to Figs. 5–7 shows that these values are much larger than we obtain in our EDPP approximation, as expected from the comparison of Eqs. (29) and (30), and in fact are close to what we obtain in our MEP model. Apparently their model predicts too much polarization and our EDPP predicts too little at high energy.

F. Inelastic cross sections

We have already described some of the predictions of the MEP model for integral inelastic cross sections in a preliminary communication of this work.⁶² In general, we do not expect as much accuracy for these cross sections as for the simpler and better studied elastic ones. In this context, Tables VII and VIII show that the MEP model predicts reasonably accurate inelastic cross sections at all energies.

VI. DISCUSSION OF MODELS

A. MEP model

From one point of view it appears that the most serious approximation in the MEP model is the representation of the dense (in fact, above the ionization potential, continuous) level structure of the helium atom by a single level. From another point of view, however, this is an advantage since a calculation with many pseudostates also has many pseudostate thresholds, each associated with an unreal resonance. Thus, to make calculations at specific energies, the basis may have to be altered to move these resonances.⁶ In actual pseudostate calculations the total inelastic cross section converges rapidly with increasing numbers of short-range pseudostates,⁶ so it is not too unrealistic to model the entire spectrum with a single pseudochannel. If we take the model literally and interpret the coupling to the pseudochannel in terms of some implicit pseudostate wave function, it is clear (since no one pseudostate yields the entire polarization potential at all r) that the pseudostate must be a function of r as well as of target coordinates. In this case there would be derivative-coupling terms arising from the operation of ∇^2 on the pseudostate. These derivative-coupling terms are not included in the present model, and their absence illustrates the

nonrigorous character of the present model. These considerations may explain in part why such a simple model is reasonably successful at predicting the total inelastic cross section, and also why the effective potential is too attractive for elastic scattering.

The results in Table VI lead to some interesting conclusions about the MEP model. For the first $N=3$ calculation we replace the single pseudochannel of our standard model by two pseudochannels, with the same excitation energy, such that the second-order adiabatic polarization potential is unchanged. This has a negligible effect on the results. In the second $N=3$ calculation we give the two pseudochannels different excitation energies. The first one is given the 2^1P excitation energy, and, since the 2^1P state contributes 35% of the static dipole polarizability,⁶³ the first state is assumed to contribute 35% of the second-order adiabatic polarization potential. Then the second state contributes the remaining 65% and its excitation energy is assigned so that the weighted average excitation energy equals the ionization potential, as in our standard model. Although this two-pseudochannel model would seem to have a much more realistic spectrum of response times, the results are again very similar to the standard model. These two checks are very encouraging.

The third $N=3$ model tests the assignment of the orbital-angular-momentum quantum number in the pseudochannel. In our standard model we made the centrifugal sudden approximation $l_2 = l_1$. In a calculation with a single pseudostate,⁴ one would have two pseudochannels with $l_j = l \pm 1$. Table VI shows that introducing a spread of orbital-angular-momentum indices does have a non-negligible effect on the results. Thus the centrifugal sudden approximation must be considered one of the most serious assumptions of the MEP model as employed here. It would be worthwhile to try to improve on this approximation in future work.

Another assumption that can be tested is Eq. (25). In general, excited states are more diffuse than the ground state, and one expects a longer-range potential in the excited state. A simple way to introduce this effect is through a scale factor, i.e., to assume

$$V_{jj}(r) = V_{11}(r/a), \quad (32)$$

where a is a scale factor. To test the sensitivity to $V_{22}(r)$, we made some calculations with $a=2$. Table VI shows that there is some sensitivity to a , but it is less than the sensitivity to l .

The MEP method is similar in some respects to the pseudostate method and the complex-optical-potential method. As compared to the pseudostate

method it has the advantage of including the full target response in the adiabatic limit at all r with only one pseudochannel, and it does not require knowledge or use of excited state or pseudostate wave functions. As compared to the method of complex optical potentials, the MEP method has the advantage of not assuming an oversimplified functional form for the absorptive interaction. Furthermore, the nonadiabatic aspects of charge polarization are modeled dynamically by the interaction of two channels in a scattering calculation rather than by an assumed velocity dependence for the optical potential. Unfortunately, the MEP model, at least in this initial trial, gives results too close to the overly attractive fully adiabatic model at low energy. It seems to do better for the elastic scattering at high energy and for the inelastic scattering at all energy.

B. EDPP model

The EDPP model is much simpler but does surprisingly well for the elastic scattering at low energy. It was never intended for use at high energy, and the present calculations confirm that it does do poorly there. The success achieved at low energy is, however, worthy of further study. Many currently popular treatments of low-energy scattering omit some combination of non-dipole effects, small- r effects, and nonadiabatic effects and succeed only when these different kinds of effects fortuitously cancel.¹⁷ Thus no single

method is successful for all the cases.¹⁷ The EDPP includes all multipoles and all ranges of r and makes an honest attempt to treat nonadiabatic effects. If a method like this is successful, it can be extended to electron-molecule scattering with more confidence than a method that relies on cancellation of errors in the atomic case.

C. Summary

Both new models presented here, the energy-dependent polarization potential and the matrix effective potential, achieve notable success for some features of the scattering but are not uniformly successful over the whole 12–400 eV range studied. Since both models are quite different from the kinds of treatments that have been widely studied and applied, it would be useful to study them further to test their *ab initio* predictive capabilities and to refine them.

ACKNOWLEDGMENTS

This work was supported in part by the National Science Foundation under Grant No. CHE77-27415. We are grateful to Dr. Trajmar, Dr. Register, and Dr. Srivastava for communicating their preliminary experimental results as well as their final ones prior to their publication. We are grateful to Dr. Hayashi and Dr. Kuchitsu for supplying their calculated results in tabular form and to Dr. Takayanagi and Dr. Callaway for comments on the manuscript.

¹See, e.g., R. Peterkop and V. Veldre, *Adv. At. Molec. Phys.* **2**, 263 (1966); D. G. Truhlar, in *Semiempirical Methods of Electronic Structure Calculations, Part B: Applications*, edited by G. A. Segal (Plenum, New York, 1977), p. 247; B. H. Bransden and M. R. C. McDowell, *Phys. Rep.* **30C**, 207 (1977); **46**, 249 (1978); N. F. Lane, *Rev. Mod. Phys.* **52**, 29 (1980).

²See, e.g., P. G. Burke and K. Smith, *Rev. Mod. Phys.* **34**, 458 (1962); K. Smith, *Calculation of Atomic Collision Processes* (Wiley, New York, 1971); S. Chung and C. C. Lin, *Phys. Rev. A* **17**, 1874 (1978).

³See, e.g., S. Geltman, in *Physics of Electronic and Atomic Collisions*, edited by T. R. Govers and F. J. deHeer (North-Holland, Amsterdam, 1972), p. 216; M. LeDourneuf, H. van Regemorter, and Vo Ky Lan, in *Electron and Photon Interactions with Atoms: Festschrift for Professor Ugo Fano*, edited by H. Kleinpoppen and M. R. C. McDowell (Plenum, New York, 1976), p. 415.

⁴K. Blum and P. G. Burke, *J. Phys. B* **8**, L410 (1975); W. C. Fon, P. G. Burke, and A. E. Kingston, *ibid.* **11**, 521 (1978); R. F. Barrett and B. A. Robson, *ibid.* **12**, 105 (1979).

⁵B. I. Schneider, *Chem. Phys. Lett.* **51**, 578 (1977).

⁶A. J. Taylor and P. G. Burke, *Proc. Phys. Soc., Lon-*

don **92**, 336 (1967); J. J. Matese and R. S. Oberoi, *Phys. Rev. A* **4**, 569 (1971); P. G. Burke and J. F. B. Mitchell, *J. Phys. B* **6**, 320 (1973); J. Callaway and J. W. Wooten, *Phys. Rev. A* **9**, 1924 (1974); J. Callaway, M. R. C. McDowell, and L. A. Morgan, *J. Phys. B* **8**, 2181 (1975); R. K. Nesbet, *Adv. Quantum Chem.* **9**, 215 (1975).

⁷R. K. Nesbet, *Phys. Rev. A* **20**, 58 (1979).

⁸M. H. Mittleman, *Ann. Phys. (N.Y.)* **14**, 91 (1961); C. J. Joachain and M. H. Mittleman, *Phys. Rev. A* **4**, 1492 (1971).

⁹R. J. Drachman and A. Temkin, in *Case Studies in Atomic Collision Physics*, edited by E. W. McDaniel and M. R. C. McDowell (North-Holland, Amsterdam, 1972), Vol. 2, p. 399.

¹⁰J. E. Purcell, R. A. Berg, and A. E. S. Green, *Phys. Rev. A* **2**, 107 (1970).

¹¹G. Csanak and H. S. Taylor, *Phys. Rev. A* **6**, 1843 (1972).

¹²J. B. Furness and I. E. McCarthy, *J. Phys. B* **6**, 2280 (1973); I. E. McCarthy, C. J. Noble, B. A. Phillips, and A. D. Turnbull, *Phys. Rev. A* **15**, 2173 (1977).

¹³K. H. Winters, C. D. Clark, B. H. Bransden, and J. P. Coleman, *J. Phys. B* **7**, 788 (1974); R. Vanderpoorten and K. H. Winters, *ibid.* **11**, 281 (1978).

- ¹⁴F. W. Byron and C. J. Joachain, in *Electron and Photon Interactions with Atoms: Festschrift for Professor Ugo Fano*, edited by H. Kleinpoppen and M. R. C. McDowell (Plenum, New York, 1976), p. 299; C. J. Joachain, R. Vanderpoorten, K. H. Winters, and F. W. Byron, Jr., *J. Phys. B* **10**, 227 (1977); R. Vanderpoorten and K. H. Winters, *ibid.* **11**, 281 (1978).
- ¹⁵D. G. Truhlar, D. A. Dixon, R. A. Eades, F. A. Van-Catledge, and K. Onda, in *Electron-Molecule and Photon-Molecule Collisions*, edited by T. N. Rescigno, V. McKoy, and B. I. Schneider (Plenum, New York, 1979), p. 151; D. G. Truhlar, K. Onda, R. A. Eades, and D. A. Dixon, *Int. J. Quantum Chem. Symp.* **13**, 601 (1979).
- ¹⁶A. Decoster, *Phys. Rev. A* **4**, 800 (1971).
- ¹⁷J. C. Callaway, *Comput. Phys. Commun.* **6**, 265 (1974).
- ¹⁸D. Andrick and H. Bitsch, *J. Phys. B* **8**, 393 (1975).
- ¹⁹H. B. Milloy and R. W. Crompton, *Phys. Rev. A* **15**, 1847 (1977).
- ²⁰H. J. Blaauw, F. J. deHeer, R. W. Wagenaar, and D. H. Barends, *J. Phys. B* **10**, L299 (1977).
- ²¹F. J. deHeer and R. H. J. Jansen, *J. Phys. B* **10**, 3741 (1977).
- ²²T. S. Stein, W. E. Kauppila, Jr., V. Pol, J. H. Smart, and G. Jeston, *Phys. Rev. A* **17**, 1600 (1978).
- ²³R. E. Kennerly and R. A. Bonham, *Phys. Rev. A* **17**, 1844 (1978).
- ²⁴J. F. Williams, *J. Phys. B* **12**, 265 (1979).
- ²⁵D. F. Register, S. Trajmar, and S. K. Srivastava, *Phys. Rev. A* **21**, 1134 (1980).
- ²⁶V. M. Martin, M. J. Seaton, and J. B. G. Wallace, *Proc. Phys. Soc., London* **72**, 701 (1958).
- ²⁷L. Castillejo, I. C. Percival, and M. J. Seaton, *Proc. Roy. Soc., London Sect. A* **254**, 259 (1960).
- ²⁸M. H. Mittleman and R. Pu, *Phys. Rev.* **126**, 370 (1962); M. H. Mittleman, *Adv. Theor. Phys.* **1**, 283 (1965).
- ²⁹A. L. Fetter and K. M. Watson, *Adv. Theor. Phys.* **1**, 115 (1965).
- ³⁰P. G. Burke, in *Atomic Collision Processes*, edited by S. Geltman, K. T. Mahanthappa, and W. E. Brittin (Gordon and Breach, New York, 1969), p. 1.
- ³¹C. J. Joachain, *Quantum Collision Theory* (North-Holland, Amsterdam, 1975), pp. 609–611.
- ³²See, e.g., K. S. Pitzer, *Quantum Chemistry* (Prentice-Hall, Englewood Cliffs, 1953), p. 504.
- ³³M. J. Seaton and L. Steenman-Clark, *J. Phys. B* **10**, 2639 (1977).
- ³⁴R. J. Drachman, *J. Phys. B* **12**, L699 (1979).
- ³⁵The energy-independent part of the r^{-6} term has been considered many times; see, e.g., A. Dalgarno and R. W. McCarroll, *Proc. R. Soc. London, Ser. A* **237**, 383 (1956); A. Dalgarno, G. W. F. Drake, and G. A. Victor, *Phys. Rev.* **176**, 194 (1968); A. Dalgarno and P. A. Shorer, *Phys. Rev. A* **20**, 1307 (1979); H. Eissa and U. Opik, *Proc. Phys. Soc., London* **92**, 556 (1967); U. Opik, *ibid.* **92**, 566 (1967); C. J. Kleinman, Y. Hahn, and L. Spruch, *Phys. Rev.* **165**, 53 (1968); and J. Callaway, R. W. LaBahn, R. T. Pu, and W. M. Duxler, *Phys. Rev.* **168**, 12 (1968).
- ³⁶K. Onda, Institute for Space and Aeronautical Science Technical Report No. 471, University of Tokyo, 1971 (unpublished).
- ³⁷D. R. Bates, in *Quantum Theory. I. Elements*, edited by D. R. Bates (Academic, New York, 1961), p. 251.
- ³⁸Reference 36 also includes another derivation that yields $6Sv^2/\omega^3r^6$ for the energy-dependent term.
- ³⁹D. G. Truhlar and N. A. Mullaney, *J. Chem. Phys.* **68**, 1574 (1978).
- ⁴⁰R. T. Pack, *J. Chem. Phys.* **60**, 633 (1974); M. A. Brandt and D. G. Truhlar, *Chem. Phys.* **13**, 461 (1976).
- ⁴¹T. G. Strand and R. A. Bonham, *J. Chem. Phys.* **40**, 1686 (1964).
- ⁴²C. C. J. Roothaan, L. M. Sachs, and A. W. Weiss, *Rev. Mod. Phys.* **32**, 191 (1960).
- ⁴³M. E. Riley and D. G. Truhlar, *J. Chem. Phys.* **63**, 2182 (1975).
- ⁴⁴A. Dalgarno and N. Lynn, *Proc. Phys. Soc., London* **A70**, 223 (1957).
- ⁴⁵A. D. Buckingham and P. G. Hibbard, *Symp. Faraday Soc.* **2**, 41 (1968).
- ⁴⁶M. A. Brandt, D. G. Truhlar, and F. A. Van-Catledge, *J. Chem. Phys.* **64**, 4957 (1976); D. G. Truhlar, N. M. Harvey, K. Onda, and M. A. Brandt, in *Algorithms and Computer Codes for Atomic and Molecular Quantum Scattering Theory*, edited by L. Thomas (National Resource for Computation in Chemistry, Lawrence Berkeley Laboratory, Berkeley, 1979), Vol. I, p. 220.
- ⁴⁷D. G. Truhlar, J. K. Rice, S. Trajmar, and D. C. Cartwright, *Chem. Phys. Lett.* **9**, 299 (1971).
- ⁴⁸M. J. Seaton, *Proc. Phys. Soc., London* **77**, 174 (1961).
- ⁴⁹L. D. Landau and E. M. Lifshitz, *Quantum Mechanics*, 2nd ed. (Pergamon, Oxford, 1965), p. 542; I. Úleha, L. Gomolčák, and Z. Pluhař, *Optical Model of the Atomic Nucleus* (Academic, New York, 1964), p. 42; R. B. Bernstein, *Adv. Chem. Phys.* **10**, 75 (1966).
- ⁵⁰R. W. LaBahn and J. Callaway, *Phys. Rev.* **180**, 91 (1969).
- ⁵¹R. W. LaBahn and J. Callaway, *Phys. Rev.* **188**, 520 (1969).
- ⁵²R. W. LaBahn and J. Callaway, *Phys. Rev. A* **2**, 366 (1970).
- ⁵³A. L. Sinfailam and R. K. Nesbet, *Phys. Rev. A* **6**, 2118 (1972).
- ⁵⁴W. M. Duxler, R. T. Poe, and R. W. LaBahn, *Phys. Rev. A* **4**, 1935 (1971).
- ⁵⁵P. G. Burke and W. D. Robb, *J. Phys. B* **5**, 44 (1972).
- ⁵⁶J. P. Bromberg, *J. Chem. Phys.* **61**, 963 (1974).
- ⁵⁷R. H. Jansen, F. J. deHeer, H. J. Luyken, B. van Wingerden, and H. J. Blaauw, *J. Phys. B* **9**, 185 (1976).
- ⁵⁸D. P. Dewangen and H. R. J. Walters, *J. Phys. B* **10**, 637 (1977).
- ⁵⁹W. C. Fon, K. A. Berrington, P. G. Burke, and A. E. Kingston, *J. Phys. B* **12**, 1861 (1979).
- ⁶⁰S. Hayashi and K. Kuchitsu, *J. Phys. Soc. Jpn.* **42**, 621 (1977).
- ⁶¹S. Hayashi and K. Kuchitsu, *Chem. Phys. Lett.* **44**, 1 (1976).
- ⁶²D. G. Truhlar and K. Onda, *Phys. Lett. A* **76**, 119 (1980).
- ⁶³P. G. Burke, J. W. Cooper, and S. Ormonde, *Phys. Rev.* **183**, 245 (1969).